Agricultural and Forest Meteorology 260–261 (2018) 154–164

Contents lists available at ScienceDirect

Agricultural and Forest Meteorology

journal homepage: www.elsevier.com/locate/agrformet

Estimating spring frost and its impact on yield across winter wheat in China

Liujun Xiao[a,b], Leilei Liu[a], Senthold Asseng[b], Yuming Xia[a], Liang Tang[a], Bing Liu[a,b], Weixing Cao[a], Yan Zhu[a,*]

[a] National Engineering and Technology Center for Information Agriculture, Jiangsu Key Laboratory for Information Agriculture, Jiangsu Collaborative Innovation Center for Modern Crop Production, Nanjing Agricultural University, Nanjing, Jiangsu, 210095, PR China

[b] Department of Agricultural and Biological Engineering, University of Florida, Gainesville, FL, 32601, USA

ARTICLE INFO

Keywords:
Climate change
Frost
Spatial and temporal variation
Yield variability
Phenology shift
Winter wheat

ABSTRACT

Frost events in spring pose a serious threat to wheat production in China. These events coincide with late vegetative stages and reproductive development, which are sensitive to frost stress. To understand the spatio-temporal pattern of spring frost and its impact on winter wheat yield, we calculated the accumulated frost degree-days (AFDD) as an index for frost risk affecting yield. Additional indices to characterize the spring frost risk included accumulated frost days and temperature-drop-rate. These indices were calculated for the growth period from stem elongation to flowering with historical data collected from 161 stations across the main winter wheat growing area in China from 1981 to 2009. Frost risk is smaller in the cooler northern and warmer southern regions than in the central winter wheat growing region of China. Huang-Huai Subregion (HHS) has the greatest frost duration, intensity and suffers the largest yield losses due to spring frost. Frost risk during stem elongation to flowering has not been significantly decreased in the winter wheat-growing regions of China under climate warming. While rising temperature reduces frost events in general, it also accelerates wheat phenology which increases the risk of spring frost. Quantifying future trends and impacts of spring frost damage on wheat production will be critical for developing appropriate adaptation and mitigation strategies for food availability in China and other regions of the world affected by frost.

1. Introduction

Extreme climate events and agricultural disasters have increased in the past decades (IPCC, 2012). Frost disaster is one of the extreme events characterized by a short duration of freezing air that is destructive to crop growth and production (Crimp et al., 2016; Frederiks et al., 2015). Frost events in spring occur frequently in many regions of the world, such as China (Li et al., 2015a; Zhong et al., 2008), United State of America (Holman et al., 2011; Whaley et al., 2004), and Australia (Zheng et al., 2015, 2012). For instance, despite a warming trend of 0.17 °C per decade since 1960, frost season length has still increased by 26 days across southern Australia and frost-related production risk has increased by as much as 30% across much of the Australian wheatbelt (Crimp et al., 2016). The relationship between a warming climate and increasing spring frost damage to crops seems like a paradox (Crimp et al., 2016; Gu et al., 2008; Li et al., 2016b). The underlying reasons are as follows: Firstly, a higher temperature accelerates vegetative development, and shifts frost-sensitive reproductive stages ahead in spring (Chen et al., 2014; Saeidi et al., 2014; Shimono, 2011; Wang et al., 2013); Secondly, complicated warm-cold fluctuations in spring may increase the uncertainty of spring frost events (Gu et al., 2008); And thirdly, the tissues and organs of winter habit cereals which experienced a warm winter are more susceptible to low temperature stress in the spring (Li et al., 2015b, 2016b).

Winter wheat (Triticum aestivum L.) is a winter habit crop which requires a low temperature to complete vernalization and can survive from some low temperature conditions during early vegetative stages (Fowler and Carles, 1979; Fowler et al., 1996). Frost tolerance of winter wheat can be acquired via freeze hardening during winter, however, it decreases rapidly through frost dehardening after crops resumed growth in spring (Bergjord et al., 2008; Frederiks et al., 2012, 2015; Fuller et al., 2009, 2007; Majláth et al., 2012). As stem extension pushing the apex above the insulating soil surface at stem elongation stage, floret primordium differentiation commences and the apex switches to the production of reproductive primordia (Whaley et al., 2004; Zhong et al., 2008), winter wheat becomes more sensitive to frost damage at this stage (Single, 1984). Spring frost damage occurs when canopy temperature fall below 0 °C or Stevenson screen air temperatures below 2 °C (Frederiks et al., 2015; Zheng et al., 2015). Rapid temperature-drop-rate can cause more severe frost damage than slow

* Corresponding author.
E-mail address: yanzhu@njau.edu.cn (Y. Zhu).

https://doi.org/10.1016/j.agrformet.2018.06.006
Received 3 October 2017; Received in revised form 5 June 2018; Accepted 6 June 2018
Available online 15 June 2018

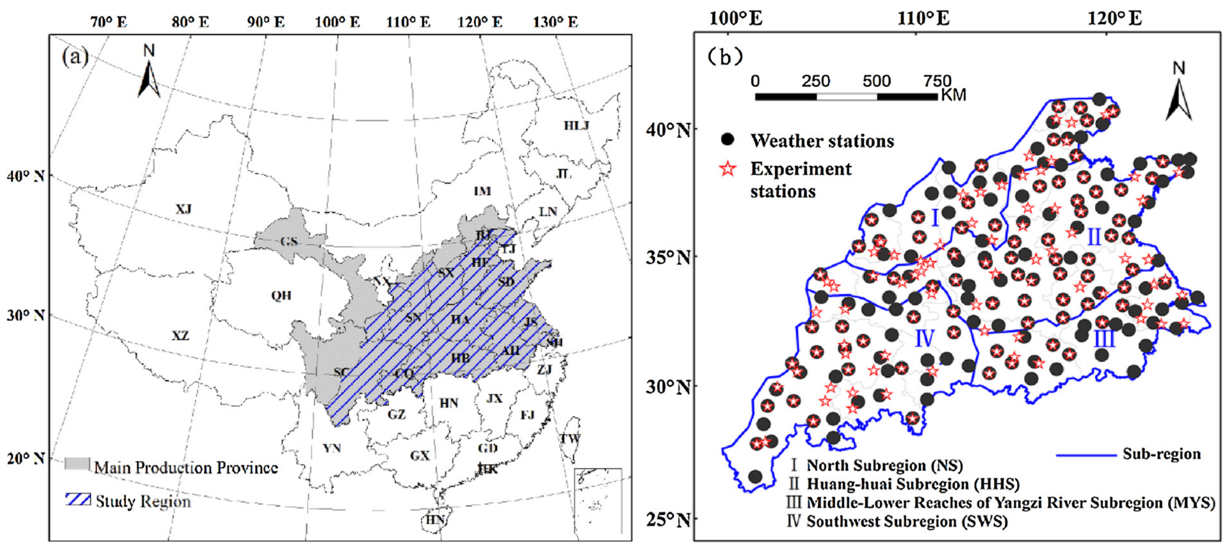

Fig. 1. (a) Map of China with main winter wheat-growing region and study region, and (b) locations of weather stations (black dots) and agro-meteorological experimental stations (red stars).

temperature-drop-rate because crops cannot acclimate to a sudden cold condition (Al-Issawi et al., 2013; Bergjord et al., 2008; Li et al., 2014). A sudden frost event at the sensitive post-stem elongation stage can cause severe yield loss (Al-Issawi et al., 2013; Fuller et al., 2007; Li et al., 2015c; Zhong et al., 2008). The spring frost stress-induced yield loss is highly correlated with the reduction of tiller and spike number, which are associated with a restriction on stem extension, specific leaf area and photosynthetic capacity (Li et al., 2015c; Valluru et al., 2012). As shown in the field experiment (2010–2011) by Li et al. (2015c), the reduction of spike number was 8%–15% and the yield loss was 5%–14% with a 5-day spring frost episode (with daily minimum temperature in the range of 0 to 4 °C) at the elongation stage. The yield loss increases with lower temperature (Wu et al., 2014). 1 °C minimum temperature drop below threshold temperature during reproductive stage could increase wheat damage from 10% to 90% (Marcellos and Single, 1984).

Winter wheat is a major staple food crop in China, accounting for more than 15% of total crop planting area and more than 20% of total crop production of China in recent years (2010–2014) (National Bureau of Statistics of China, 2015), which makes China the largest producer of wheat in the world (FAO, 2016) (last visited 11 May 2018). Winter wheat is typically sown in autumn, growing through winter and harvested in the following summer in China (Jin, 1996). Previous studies have been widely concerned with the spatio-temporal patterns of spring frost in China in recent decades (Li et al., 2015a; Yue et al., 2016; Zhong et al., 2007a,b). Spring frost widely distributes in about 85% of the total winter wheat planting area in China (Yue et al., 2016). It usually occurs in March and April during the immature ear and early ear emergence period, nevertheless, the frost damage to winter wheat after flowering is uncommon (Li et al., 2015a; Wu et al., 2014). Huang-Huai winter wheat growing region (110 °E-118 °E and 34 °N-36 °N) suffers the most severe spring frosts in China (Feng et al., 1999). In this region, the probability of spring frost has been increasing since the 1970 s (Zhong et al., 2007b). In eastern China, spring frost events are frequent in the north of Huaihe river valley (31 °N–36 °N) and the historical occurrence cycles of the spring frost is 22 years, 11 years, 4 years and 2 years depending on different stations (Bao et al., 2012). The average wheat grain yield variations caused by single spring frost in each decade during 1961–2000, ranged between -20.87% and 3.43%, based on six agro-meteorological stations in Eastern China (Li et al., 2015a). Previous studies have characterized the spatio-temporal distribution of extreme temperature events, drought events, and their impacts on wheat yield in different areas (Liu et al., 2014; Tao et al., 2015; Wang et al., 2016; Zhang et al., 2014). Heat stress and drought could occur after spring frost events, which would further aggravate the negative impacts on grain yield (Zheng et al., 2012). However, few studies have quantified the impacts of both types of climatic variables, and separate the spring frost impact from other climatic stress impacts on winter wheat production using long-term historical climate and yield records at a large spatial scale. Furthermore, the advancement of the elongation and heading stages caused by climate warming has played an important role in increasing the risk of spring frost (Gu et al., 2008; Zheng et al., 2012). Previous frost risk assessments often used fixed wheat growth seasons among different years and less considered actual temporal phenology variation among different ecological regions (Yue et al., 2016; Zhong et al., 2007a). Therefore, using historical observed phenology dates and climate records to analyze the spatio-temporal variability of spring frost, and separate its impacts from other extreme climate conditions on wheat yield in China is critical for preparing adaptation strategies to minimize the impacts of frost on food supply and regional food availability.

In this study, the main objectives are the following: 1) to calculate frost indices from daily minimum temperature records between stem elongation and flowering stage across the main winter wheat-growing region of China; 2) to analyze the spatial and temporal variation of frost during 1981–2009; and 3) to investigate the relationship between agro-climatic variation and grain yield variability, and separate the impact of spring frost on winter wheat yield from other climate factors.

2. Materials and methods

2.1. Study region and data source

The study region is located in the main winter wheat-growing region of China (26°13′-40°68′N, 100°83′-121°87′E), which contributes to more than 83% of the total wheat planting area and 88% of total wheat production in China (National Bureau of Statistics of China, 2015) (Fig. 1a). The whole region includes 14 main winter wheat production provinces and municipalities. Spring wheat-growing regions (Fig. 1a grey) were removed according to Chinese wheat planting regionalization (Jin, 1996). The whole study region is divided into four sub-regions (Fig. 1b) based on geographical environment and climate condition, including two northern sub-regions, the North Subregion (NS) and the Huang-Huai Subregion (HHS), and two southern sub-regions, the Middle-Lower Reaches of Yangzi River Subregion (MYS) and the Southwest Subregion (SWS) (Jin, 1996), which are the same as Liu et al (2014).

Table 1
Dataset used in this study.

Dataset	Dataset description	Objective	Source
Historical daily weather data	Daily maximum temperature Daily minimum temperature Daily sunshine hour Daily precipitation	Calculating the value of spring frost indices from stem elongation to flowering each year; Estimating the climate-yield relationship and spring frost impact on grain yield	China meteorological administration (161 weather stations)
Winter wheat experimental data	Phenological date	Measuring the period from stem elongation to flowering	China meteorological administration (141 agro-meteorological experimental stations)
	Phenological date Grain yield	Estimating the climate- yield relationship and spring frost impact on grain yield	China meteorological administration (81 agro-meteorological experimental stations)

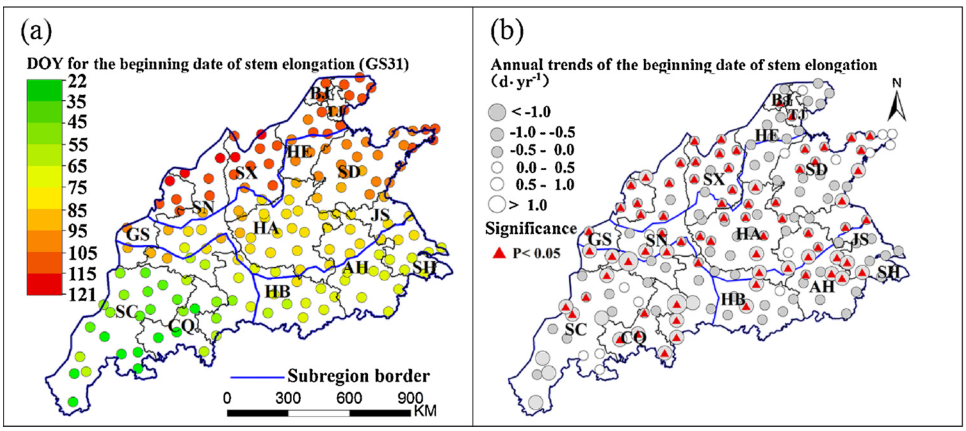

Fig. 2. Average day of year (DOY) for the beginning date of stem elongation (a) during 1981–2009, and its annual trend (b) at each station. The beginning date of stem elongation was recorded at Zadoks scale GS31 when the 1 st node was detectable. In Fig. 2(b), temporal trend of observed date of the beginning of stem elongation from 1981 to 2009 at each station was fitted with simple linear regression; the size of the circle represents the magnitude of linear regression coefficient; grey and white circles indicate negative and positive regression coefficients, respectively; red triangles indicate the significant correlation at 0.05 levels.

A total of 161 weather stations and 141 national agro-meteorological experimental stations were chosen for calculating frost stress indices in this study (Table 1). The weather stations were distributed throughout the entire study region. The observed daily weather data including minimum and maximum air temperature, sunshine hour, and precipitation at 161 weather stations (Fig. 1b, Table 1) from 1981 to 2009 can be obtained from the Chinese Meteorological Administration (CMA). The Angstrom-Prescott model was used to calculate daily solar radiation data based on daily sunshine hours (Prescott, 1940). Observed winter wheat phenological dates at 141 stations were obtained from national agro-meteorological experimental stations (AES) (Fig. 1b). These AES were built in consideration of the geographical and climatological difference. Phenological dates at other 20 stations without an agro-meteorological experimental station were replaced by the phenological dates of the best-fitted nearby AES. The phenological records included the dates of major crop phenological events since 1980, such as sowing, the beginning date of stem elongation, heading, flowering, and maturity. The agricultural phenological dates were collected by well-trained agricultural technicians at each station. Fig. 2(a) shows the average values of the day of year (DOY) for the beginning date of stem elongation during 1981–2009. Obvious differences of the beginning date of stem elongation were observed in different sub-regions. The maximum difference in the beginning date of stem elongation across the whole study region was 98 days. Temporal trend of observed phenological date from 1981 to 2009 at each station was fitted with simple linear regression. Significant advanced trends ($p < 0.05$) were observed at 45.3% of stations for the beginning date of stem elongation, and the average advanced time at these stations was 0.5 d y^{-1} (Fig. 2b).

Owing to the limited yield records among 141 agro-meteorological experimental stations, we selected 86 available stations (Table 1, Fig. S1) from them with more than 20-year records of winter wheat grain yields and agronomic management practices to investigate the climate-wheat yield relationship and spring frost impact on winter wheat yield. Grain yields, growing period length and weather conditions during growing season at these 86 stations of each sub-region are shown in Table 3 and Fig. S1. These agro-meteorological stations supported by CMA generally perform the optimum management practices based on the local conventional agriculture practices, including fertilization and irrigation (several times every year), pesticide applications, and weed control for crop development at these experiments (Tao et al., 2017; Zhang et al., 2010).

2.2. Analysis method

2.2.1. Frost stress indices

A threshold (Th) of 2 °C in air temperature (mostly measured at a 2 m height) was used to define spring frost events; this measurement is consistent with previous studies (Crimp et al., 2014, 2016; Zheng et al., 2015). To estimate the sensitivity of spring frost with different threshold, a range of damage threshold temperatures from −2 °C to 2 °C was also tested.

The study period was defined as the spring frost sensitivity window from beginning of stem elongation (Zadoks stages GS31) to flowering (Zadoks stages GS65) for each year in this study, supported by previous studies in China (Li et al., 2015a; Wu et al., 2014; Zhong et al., 2008, 2007b). The study periods varying between years and stations were applied to calculate frost indices in the study region from 1981 to 2009. Average study period and probability distribution of observed frost event (T_{min} < 2 °C) for the entire region during 1981–2009 are shown in Fig. 3

Three frost indices including accumulated frost days (AFD), accumulated frost degree-days (AFDD), and temperature-drop-rate (TDR) were calculated with daily minimum air temperature from stem elongation to flowering, as summarized in Table 2. Accumulated frost days (AFD), which measures duration of frost, was defined as accumulated days when $T_{min} \leq T_h$ from stem elongation to flowering. The accumulated frost degree-days (AFDD) was defined as the cumulative temperature lower than frost threshold throughout the study period, accounting for both duration and the magnitude of frost stress. Temperature-drop-rate (TDR) was defined to measure the temperature

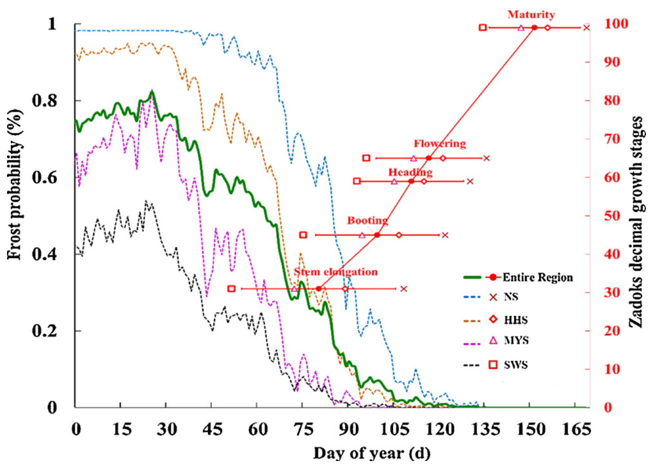

Fig. 3. The average probability distribution of observed frost event ($T_{min} < 2$ °C) for the entire region (green solid line) and four sub-regions (dashed line) during 1981–2009. The right Y-axis (red) is the Zadoks growth scale. At each stage, the red furcation, prismatic, triangle, square and dot represent the average phenology dates (stem elongation, booting, heading, flowering, and maturity) in NS (North Subregion), HHS (Huang-Huai Subregion), MYS (Middle-Lower Reaches of Yangzi River Subregion), SWS (Southwest Subregion) and the Entire Region, respectively. The horizontal error bars indicate the average phenology date ± SD for the Entire Region.

drop rate during one consecutive cooling period (T_{min} at any day of one consecutive cooling period always lower than T_{min} at previous day) when frost occurs ($T_{min} < T_h$) between stem elongation and flowering.

2.2.2. Spatial and temporal variations of frost from stem elongation to flowering

To show the spatial variation of spring frost in the study region, the average and maximum values of each index from stem elongation to flowering for each station during 1981–2009 were calculated. The spatial characteristics of each frost index were displayed as maps by using the spatial interpolation of Ordinary Kriging in ArcGIS 9.3 (Mueller et al., 2004).

The temporal trends from 1981 to 2009 of each frost index at each sub-region were fitted with linear regression. In addition, the annual trends among the four sub-regions were calculated by fitting a time series of each index over all stations in each sub-region from 1981 to 2009.

2.2.3. Effects of phenology shift on temporal trends of spring frost

$Trend_{obs}$ was defined as the trend of frost indices calculated based on the observed phenological dates of the study period and daily minimum temperature at each station; thus, $Trend_{obs}$ was jointly affected by the variation of minimum air temperature and phenology shift during 1981–2009. In order to separate the effect of phenology shift from the confounding effects that affect $Trend_{obs}$, the trend of frost affected only by the variation of minimum air temperature ($Trend_{tem}$) needs to be quantified first. Therefore, $Trend_{tem}$ in each year was recalculated with a fixed calendar date, which was a fixed phenological range from the average stem elongation dates of 1981–2009 (Fig. 2a) to the average flowering dates of 1981–2009. The difference between $Trend_{obs}$ and $Trend_{tem}$ generally represents the effects of phenology shift on annual trend of frost ($Trend_{phe}$) during 1981–2009. $Trend_{obs}$, $Trend_{tem}$, and $Trend_{phe}$ at each station of the sub-region were fitted with linear regression and then tested by a paired *t*-test ($p < 0.05$ and $p < 0.01$) at each station and each sub-region.

Table 3
Observed weather conditions, period lengths during the growing season (from emerging to mature) and grain yields from 86 agro-meteorological experimental stations across four sub-regions during 1981–2009. Values are shown as mean ± standard error of the mean (s.e.).

Sub-region	Average temperature (°C)	Total precipitation (mm)	Growing period length (d)	Yield (t/ha)
NS	7.4 ± 1.1	170 ± 76	255 ± 13	4.5 ± 1.7
HHS	9.2 ± 1.2	226 ± 107	229 ± 18	5.2 ± 1.8
MYS	10.5 ± 1.0	254 ± 186	200 ± 14	4.1 ± 1.5
SWS	11.6 ± 1.3	408 ± 129	190 ± 17	3.8 ± 1.4

NS, the North Subregion, HHS, the Huang-Huai Subregion, MYS, the Middle-Lower Reaches of Yangzi River Subregion, SWS, the Southwest Subregion.

2.2.4. Impact of spring frost on wheat grain yield

Temperature, including normal and extreme temperatures, is critical limiting factor for grain yields (Liu et al., 2014; Schauberger et al., 2017; Zhang et al., 2017a). To separate the effect of spring frost stress on grain yield from normal temperature and heat stress effects during 1981–2009, we applied a multivariate regression analysis (Eq. (1)) across different sub-regions (Table 3) with all the stations, following the approach by previous studies (Liu et al., 2013; Lobell et al., 2011; Wang et al., 2014). Accumulated frost degree-days (AFDD), growing-degree-days (GDD) and heat-degree-days (HDD) were used to capture the effects of frost stress, normal temperature and heat stress on wheat grain yields, respectively.

$$\text{Type I}: \ Log(Y_{i,t}) = \beta_0 + \beta_{AFDD,GP}\mathrm{AFDD}_{i,t,GP} + \beta_{GDD,GP}\mathrm{GDD}_{i,t,GP} + \beta_{HDD,GP}\mathrm{HDD}_{i,t,GP} + \beta_i \mathrm{station} + \beta_t t + \varepsilon_{i,t} \quad (1)$$

where $Y_{i,t}$ is the yield in the station *i* and year *t*, log is the natural logarithm; AFDD is the accumulated frost degree-days in Table 2; Growth period (GP) represents three crop growth stages: early growth from emerging to stem elongation (GP1), reproductive period from elongation to flowering (GP2), and grain-fill from flowering to mature (GP3); For each growth stage, GDD is the sum of growing degree days between 2 °C and 30 °C, and HDD is the sum of growing degree days above 30 °C; the frost threshold temperatures (from −8 °C to 6 °C with interval of 1 °C) in three-growth periods were used to calculate AFDD

Table 2
Definition of frost indices.

Index (unit)	Term	Formula[a]	Definition
AFD (d)	Accumulated frost days		Accumulated frost days with daily minimum air temperature below 2 °C from stem elongation (Zadoks stages GS31) to flowering (Zadoks stages GS65)
AFDD (°C•d)	Accumulated frost degree-days	$\sum_{ds}^{df} \mathrm{MAX}\,(T_h - T_{min}, 0)$	Accumulated frost degree-days from stem elongation (ds) to flowering (df) which represents the comprehensive effects of duration and intensity
TDR (°C•d^{-1})	Temperature-drop-rate	$\mathrm{Mean}\left(\frac{T_{min\,d1} - T_{min\,dk}}{d1 - dk}\right)$	The average value of TDR during all the consecutive cooling period (T_{min} at any day of one consecutive cooling period always lower than T_{min} at previous day)

[a] T_h is temperature threshold of spring frost (2 °C), $T_{min,i}$ represents daily minimum air temperature on day i; ds represents the begining of stem elongation; df represents flowering; *d1* represents the first day of one cooling period; *dk* represents the day when T_{min} is lowest during one cooling period; for each consecutive cooling period: $T_{min\,dk} < T_{min\,d1} < 2$.

and test the best model; β_0 represents an intercept. $\beta_{indeces,GP}$ are model coefficients for log yield in response to climate indices (GDD, AFDD, HDD) at one growth period (GP); β_0 represents an intercept associated with stations to capture station-specific fixed effects; β_t represents the sub-region-specific linear trend to capture the effects of varieties and technology improvements on observed yield during the study period; $\varepsilon_{i,t}$ represents the residual error.

Previous researches have demonstrated precipitation and solar radiation were key factors affecting crop yield variability (Tao et al., 2017, 2016; Zhang et al., 2010), and wheat could suffer cumulative damage when heat and drought events occur during or after spring frost events (Barlow et al., 2013; Zheng et al., 2012). To further capture the effects of other climate stresses during different growth stages on wheat grain yields and separate the impacts of spring frost from them, we carried out the multiple linear regression model (Eq. (2)) and linear mixed model (Eq. (3)) for temperature, precipitation, and solar radiation.

$$\text{Type II: } Log(Y_{i,t}) = \beta_0 + \beta_{AFDD,GP}\text{AFDD}_{i,t,GP} + \beta_{GDD,GP}\text{GDD}_{i,t,GP} + \beta_{HDD,GP}\text{HDD}_{i,t,GP} + \beta_{SRD,GP}SRD_{i,t,GP} + \beta_{P,GP}\text{P}_{i,t,GP} + \beta_{i,GP}\text{station} + \beta_{t,GP}\text{t} + \varepsilon_{i,t} \quad (2)$$

$$\text{Type III: } Log(Y_{i,t}) = \beta_0 + \beta_{AFDD}\text{AFDD}_{i,t,GP} + \beta_{GDD}\text{GDD}_{i,t,GP} + \beta_{HDD}\text{HDD}_{i,t,GP} + \beta_{SRD}SRD_{i,t,GP} + \beta_{P}\text{P}_{i,t,GP} + \beta_{random,i}\text{station} + \beta_{random,t}\text{t} + \varepsilon_{i,t} \quad (3)$$

where $Y_{i,t}$, β_0, β_t, β_s, i, t, $\beta_{AFDD,GP}$, $\beta_{GDD,GP}$, $\beta_{HDD,GP}$ and $\varepsilon_{i,t}$ are the same as type I (Eq. (1)); we considered more climate variables, including solar radiation (SRD) and accumulated precipitation (P). For comparison, we applied a linear mixed model (type III) as proposed by Carter et al. (2016). For type III, the coefficients of station and year are treated as random effects, and other variables and parameters are the same as type II. Furthermore, we carried out a regression with linear and quadratic terms for time trends to capture technology change. Results were similar and model performances were not obviously improved when using quadratic terms for time trends. Note that nearly identical results between linear and polynomial models were also reported by previous studies and the non-linear eff ;ects of technology improvement and human management on crop yields could not be completely explained even though using polynomial function of time series to fit the model (Schauberger et al., 2017; Schlenker and Roberts, 2009; Zhang et al., 2018). To simplify our model structure we did not include non-linear eff ;ects of time trends in our final analyses.

To test the influence of multicollinearity among the input variables before model fitting, we calculated correlation coefficients among predictor variables as shown in Fig. S5 and calculated the variance inflation factor (VIF) on all predictors variables as shown in Table S3 (new). The goodness of fit was evaluated using the coefficient of determination (R^2). Leave-one-out cross-validation (LOOCV, Stone, 1974) and Akaike's Information Criterion (AIC, Akaike, 1987) were calculated for all possible input variables among three types of models to identify the most influential predictor climate variable and select the best model. To determine the frost thresholds used in this study, we checked different low temperature thresholds (from −8 °C to 6 °C with interval of 1 °C) in three-growth periods to test the model performance by using LOOCV method. LOOCV method randomly splits the data of each sub-region into K groups (K = the number of observations), fits the data on K − 1 of the groups, and evaluates prediction error on the group that was left out. The optimal low temperature threshold was determined according to the lowest root mean squared prediction error (RMSPE) from LOOCV, following the approach by Schlenker et al. (2009) and Shi et al. (2015). To further obtain the more robust model coefficients and select the best combinations of input variables, we also use stepwise function for each multiple models and get the same coefficient of AFDD from elongation to flowering. Validation measurements were done with the function cv.glm, glm, predict.glm, and step.glm in R language (Version 3.4.1).

$$R^2 = \left(\frac{\sum (P-\bar{P})(O-\bar{O})}{\sqrt{\sum (P-\bar{P})^2}\sqrt{\sum (O-\bar{O})^2}}\right)^2 \quad (4)$$

$$\text{RMSPE} = \sqrt{\frac{1}{\text{k}}\sum_1^k (P_i - O_i)^2} \quad (5)$$

where O and P are the observed and estimated values, respectively; $\bar{O}$ and $\bar{P}$ express the mean of observed and estimated values, respectively; O_i and P_i is the observed and estimated values on each one group that was left out in LOOCV system, respectively.

In order to estimate the uncertainties from the limited historical sample size and three types of model, a bootstrap resampling approach (Tao et al., 2013) was used for each sub-region. At each case, 1000 bootstrap resamples were performed for three types of model, and the median value was used as each regression coefficient.

The estimated grain yield responses to spring frost during 1981–2009 were closely represented by β_{AFDD} from elongation to flowering (GP2). The yield change with per unit change of climate index was calculated by exp (β_{index})-1 (Schauberger et al., 2017). The relative contribution of spring frost to yield (%/year) for each sub-region was calculated by multiplying estimated yields changes to spring frost (exp (β_{index})-1) with the historical annual values of AFDD during the study period (n years).

$$\text{contribution} = (\exp(\beta_{AFDD}) - 1)*\frac{1}{\text{n}}\sum_1^n AFDD \quad (6)$$

3. Results

3.1. Spatial variation of spring frost

Spatial variation of spring frost stress during the study growth stage (stem elongation to flowering) from 1981 to 2009 is shown in Fig. 4. The average values of accumulated frost days (AFD) and accumulated frost degree-days (AFDD) from stem elongation to flowering were greater in HHS and east part of SWS. During 1981–2009, the average value of accumulated frost days (AFD) from stem elongation to flowering was 2.0 days (d) in HHS and 1.8 days in MYS, which were approximately 1d higher than those in NS. Similar results were found in average values of accumulated frost degree-days (AFDD) from stem elongation to flowering during 1981–2009. In NS, there was less spring frost occurred during stem elongation to flowering, with the average AFDD less than 0.6 °C d (Fig. 4b). The average values of temperature-drop-rate (TDR) from stem elongation to flowering were generally higher in two northern regions than in two southern regions.

Similar spatial distribution but larger variation was found in the maximum values of three frost indices than those in the average values (Fig. 4d–f). The most severe frost with the highest value of all three indices was observed in the central area of HHS, with the maximum values of 10.8 d for accumulated frost days (AFD), 20.7 °C·d for accumulated frost degree days (AFDD), and 6.3 °C·d^{-1} for temperature-drop-rate (TDR). The maximum value of AFD in MYS was 10.6 days (d), while it was 9.2 d in the SYS; these values were 7.1 d and 5.7 d higher than those of the NS. The maximum values of temperature change rate (TDR) in two northern regions were approximately 1.5 °C·d^{-1} higher than those in the two southern regions.

3.2. Temporal trends of spring frost during 1981–2009

Fig. 5 shows the temporal trends during 1981–2009 for all frost indices based on the actual observed phenological dates from stem elongation to flowering. Due to the joint effects of temperature change and phenology shift, spring frost duration and intensity increased at

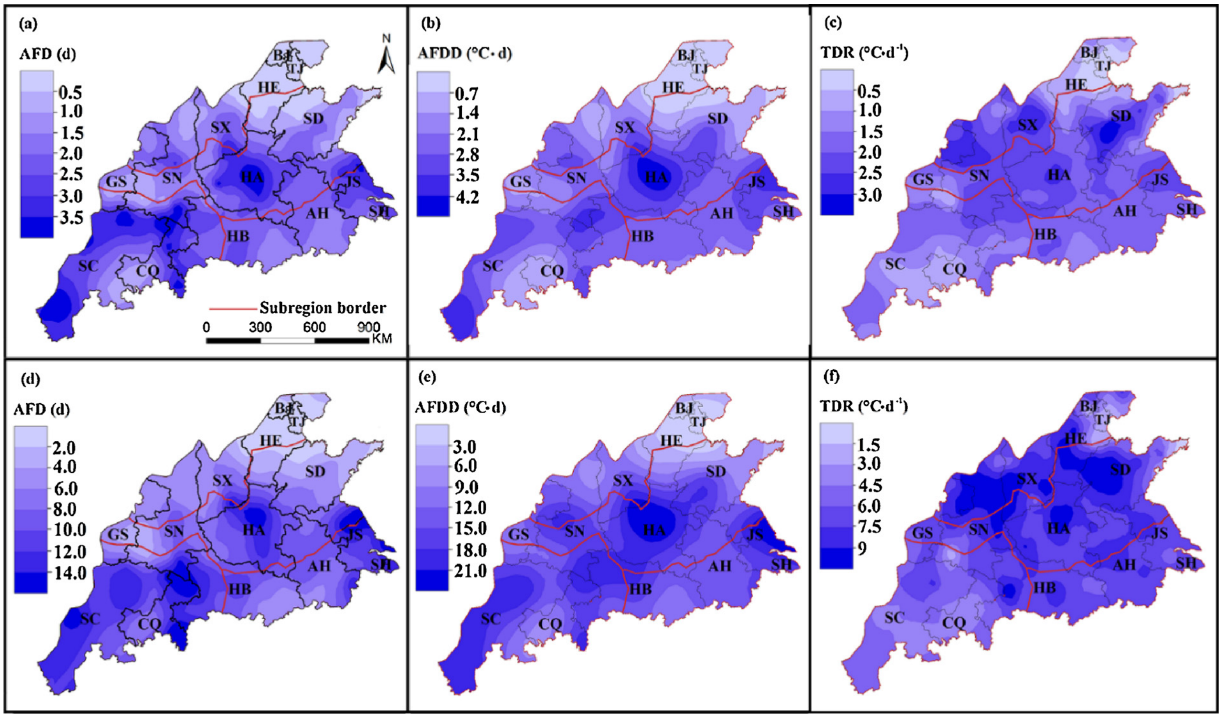

Fig. 4. Spatial variation of average (a–c) and maximum values (d–f) of spring frost indices from stem elongation (Zadoks stages GS31) to flowering (Zadoks stages GS65) during 1981–2009 across the main winter wheat-growing region of China. AFD, accumulated frost days; AFDD, accumulated frost degree-days; TDR, average drop rate of minimum temperature during spring frost events.

45.9% and 44.1% of the stations, mostly in HHS and SWS (Fig. 5a-b). In these regions, the average value increased up to 0.07 $d \cdot y^{-1}$ for accumulated frost days (AFD) and 0.10 $°C \cdot d \cdot y^{-1}$ for accumulated frost degree-days (AFDD). However, there was still a decreasing trend of spring frost duration at 47.2% of stations and of spring frost intensity at 45.3% of stations. More than half of the stations showed an increasing trend for temperature-drop-rate (TDR) for the entire region (Fig. 5c). Particularly, spring frost was expanding to the south. In most of Anhui (AH) and Jiangsu (JS) provinces, the spring frost duration and intensity and temperature-drop-rate all increased.

Temperature change during 1981–2009 decreased spring frost in most of the winter wheat-growing region (Fig. 6 a–c). However, about half of the regions had a positive trend of frost stress (Fig. 5a–c), as the effects of phenology shifting increased the trend of spring frost (Fig. 6 d–f). $Trend_{phe}$ for AFD, AFDD, and TDR increased by 0.040 $d \cdot y^{-1}$, 0.06 $°C \cdot d \cdot y^{-1}$, and 0.03 $°C \cdot d^{-1} \cdot y^{-1}$ in most parts of the study region from 1981 to 2009, respectively. The regions where $Trend_{phe}$ for AFD was more than 0.06 $d \cdot y^{-1}$ and TDR was more than 0.08 $°C \cdot d^{-1} \cdot y^{-1}$ during 1981–2009 were in Henan province (HA, central of HHS), Anhui, and Jiangsu province (HA, JS, east of MYS) due to the effects of the phenology shift.

3.3. Differences between sub-regions in temporal trend of spring frost during 1981–2009

With the single effects of variations in minimum temperature, spring frost trends generally decreased significantly for AFD in the whole region, and for AFDD and TDR in the northern two sub-regions from 1981 to 2009 (Table 4). However, the effects of phenology shift had the inverse effect on spring frost trend, which significantly increased AFD, AFDD, and TDR in most of the sub-regions. $Trend_{phe}$ for AFD and AFDD in HHS and SWS were 0.02 $d \cdot y^{-1}$ and 0.04 $C \cdot d \cdot y^{-1}$ higher than the other two sub-regions (Table 4). The phenology shift during 1981–2009 increased the temperature-drop-rate (TDR) the most in MYS. Due to the counteracted effects of temperature change and phenology shift, the actual trend of frost ($Trend_{obs}$) for AFD and AFDD showed no significant difference across four sub-regions, even though HHS and MYS had significantly increased TDR (Table 4). In the entire region, the $Trend_{obs}$

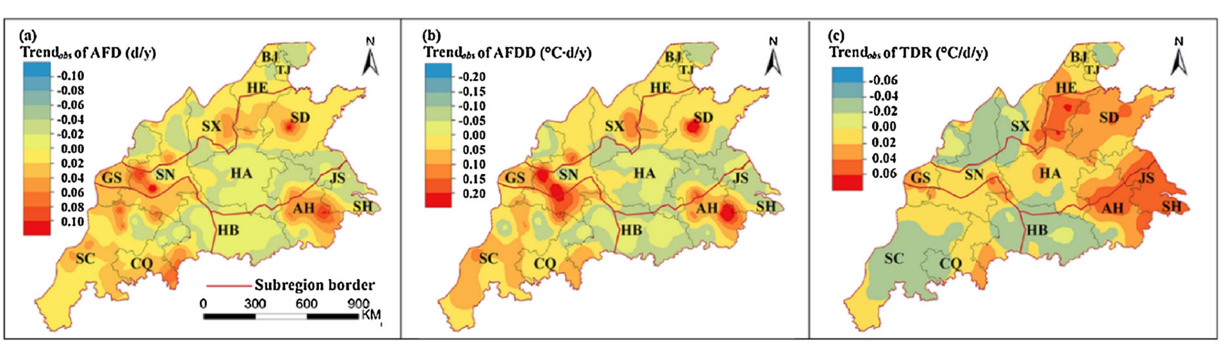

Fig. 5. Temporal trends of spring frost indices from stem elongation to flowering during 1981–2009. $Trend_{obs}$ (frost calculated during the observed phenological range between stem elongation and flowering) of AFD (accumulated frost days), $Trend_{obs}$ of AFDD (accumulated frost degree-days) and $Trend_{obs}$ of TDR (temperature-drop-rate) are shown.

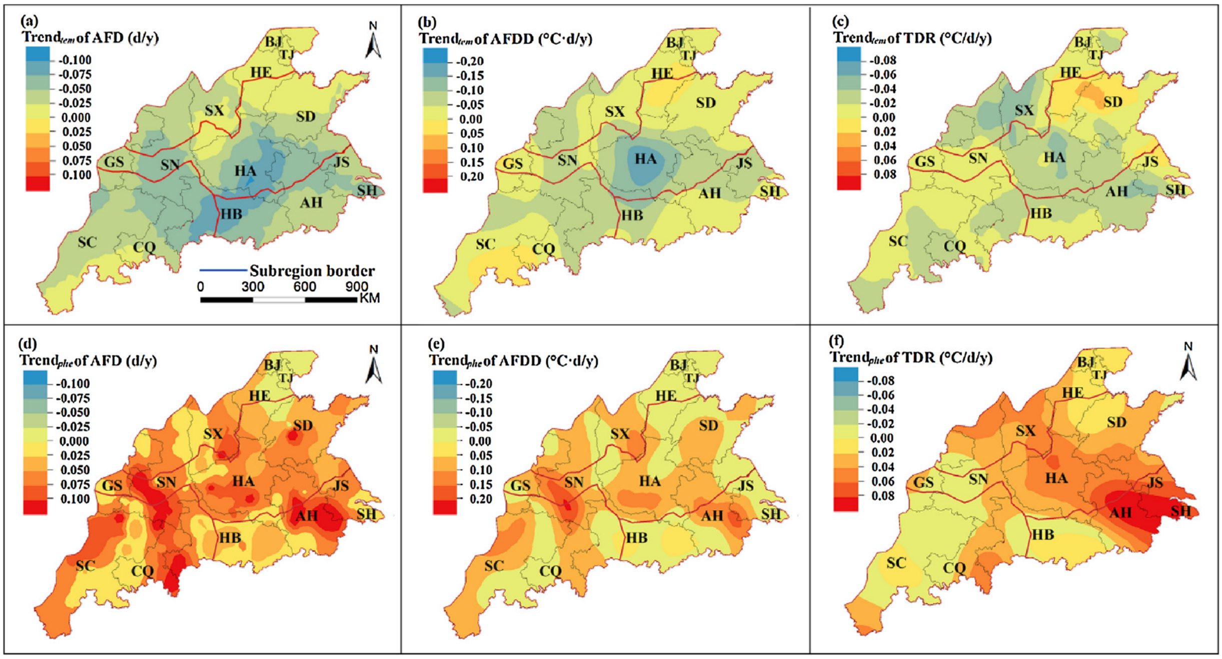

Fig. 6. Effects of temperature change and phenology shift on temporal trends of spring frost indices from stem elongation to flowering during 1981–2009. Trend$_{tem}$ (trend in minimum air temperature during a calendar period) of AFD (accumulated frost days), Trend$_{tem}$ of AFDD (accumulated frost degree-days) and Trend$_{tem}$ of TDR (temperature-drop-rate) are shown. Trend$_{phe}$ is the difference between Trend$_{obs}$ and Trend$_{tem}$.

Table 4
The temporal trends of frost indices (T_{min} < 2 °C) affected by different influencing factors in each sub-region.

Index (unit of trend)	Sub-regions	Trend$_{obs}$	Trend$_{tem}$	Trend$_{phe}$
AFD ($d{\cdot}y^{-1}$)	NS	0.007	−0.028**	0.035**
	HHS	0.005	−0.043**	0.048**
	MYS	−0.006	−0.045**	0.039**
	SWS	0.017	−0.042**	0.059**
AFFD (°C$\cdot d{\cdot}y^{-1}$)	NS	0.018	−0.047*	0.063**
	HHS	0.03	−0.054*	0.083**
	MYS	0.002	−0.027	0.029
	SWS	0.03	−0.056	0.084**
TDR (°C$\cdot d^{-1}{\cdot}y^{-1}$)	NS	−0.003	−0.031**	0.025**
	HHS	0.023**	−0.014*	0.036**
	MYS	0.030**	−0.025**	0.053**
	SWS	0.001	−0.013	0.013*

Trend$_{obs}$ (frost calculated during the observed phenological range between stem elongation and flowering) of AFD (accumulated frost days), Trend$_{obs}$ of AFDD (accumulated frost degree-days) and Trend$_{obs}$ of TDR (temperature-drop-rate) are shown. Trend$_{tem}$ (trend in minimum air temperature during a calendar period) of AFD (accumulated frost days), Trend$_{tem}$ of AFDD (accumulated frost degree-days) and Trend$_{tem}$ of TDR (temperature-drop-rate) are shown. Trend$_{phe}$ is the difference between Trend$_{obs}$ and Trend$_{tem}$. NS, the North Subregion, HHS, the Huang-Huai Subregion, MYS, the Middle-Lower Reaches of Yangzi River Subregion, SWS, the Southwest Subregion. Statistical significance was all tested using the two-tailed *t*-test. *indicates correlations significance at $p < 0.05$; ** indicates correlations significance at $p < 0.01$.

changed by -0.091 to 0.093 $d{\cdot}y^{-1}$ for AFD, -0.13 to 0.15 °C$\cdot d{\cdot}y^{-1}$ for AFDD, and -0.07 to 0.11 °C$\cdot d^{-1}{\cdot}y^{-1}$ for TDR during 1981–2009 (Fig. S3).

3.4. The impacts of spring frost on grain yield

Yield response to frost variation was estimated by only considering temperature effects with fixed linear model (type I), and by considering temperature, radiation, and precipitation effects with fixed linear model (type II) and mixed linear model (type III). As shown in Table 5, spring frost posed significant negative effects on grain yield in most of the wheat-growing regions during 1981–2009 from the coefficient estimates of three models. By comparing the determination coefficient of yield response (R^2), the statistical model of type III has the better explanation than other two types.

The sensitivities of grain yield to temperature variables were determined by the median estimates of regression coefficients (β_{AFDD}) at each station of four sub-regions during 1981–2009. As shown in Table 5 and Fig. 7, three types of model capture the similar yield responses to spring frost. HHS was the most vulnerable region to frost among the four sub-regions, where yield was estimated to decrease by about 1.5%–2.1% for each 1 °C·d increase in AFDD with three types of yield response models (Table 5). The grain yield's sensitivity to spring frost in the HHS is more than twice than SWS. The estimated contribution of spring frost to winter wheat yield depends on both the sensitivity of yield to spring frost and the historical accumulated frost degree-days. HHS (with about 5% yield losses per year) was expected to have larger yield reduction due to spring frost than other regions during 1981–2009 (Fig. 8).

4. Discussion

4.1. Temperature thresholds of spring frost

There are generally two approaches to investigating crop response to frost. The first is to design specific experiments through controlled conditions to understand the relevant frost-related mechanisms and the interactions of other stress factors (Frederiks et al., 2012, 2015; Fuller et al., 2009, 2007). The second approach is a regional assessment, which based on a large sample of observations where the individual responses to frost can be estimated with a statistical approach (such as a panel regression model or a linear mixed-model) or a process-based crop model (such as APSIM-Wheat) (Carter et al., 2016; Crimp et al., 2016; Tack et al., 2015; Zheng et al., 2015). Based on worldwide experimental studies, the wheat tissue frost damage occurs when temperature falls below the freezing temperature 0 °C (Chen et al., 2014; Porter and Gawith, 1999; Single, 1966, 1984). Some isolated experimental results have shown that the actual frost damaging temperature cannot precisely be identified by using 0 °C (Frederiks et al., 2015).

Table 5
Regression coefficients for log yield in response to AFDD and determination coefficients (R^2) from multiple linear models.

Sub-regions	Coefficient estimates (Type I)		Coefficient estimates (Type II)		Coefficient estimates (Type III)	
	β_{AFDD}	R^2	β_{AFDD}	R^2	β_{AFDD}	R^2
NS	−0.010*	0.14	−0.011*	0.27	−0.003	0.61
HHS	−0.015**	0.29	−0.021**	0.28	−0.017**	0.42
MYS	−0.009	0.30	−0.012	0.43	−0.011**	0.64
SWS	−0.007**	0.21	−0.006*	0.33	−0.005**	0.62
ES	−0.007**	0.19	−0.007**	0.21	−0.007**	0.58

β_{AFDD} are the coefficients for AFDD (T_{min} < 2 °C) in three types of the yield response model (Eq. (1)–(3)), which represent the sensitivities of grain yield to spring frost. AFDD is the accumulated frost degree-days from stem elongation (Zadoks stages GS31) to flowering (Zadoks stages GS65). NS, the North Subregion, HHS, the Huang-Huai Subregion, MYS, the Middle-Lower Reaches of Yangzi River Subregion, SWS, the Southwest Subregion, ES, the entire region. R^2 is the determination coefficient of each yield response model. *indicates significance at $p < 0.05$; ** indicates significance at $p < 0.01$.

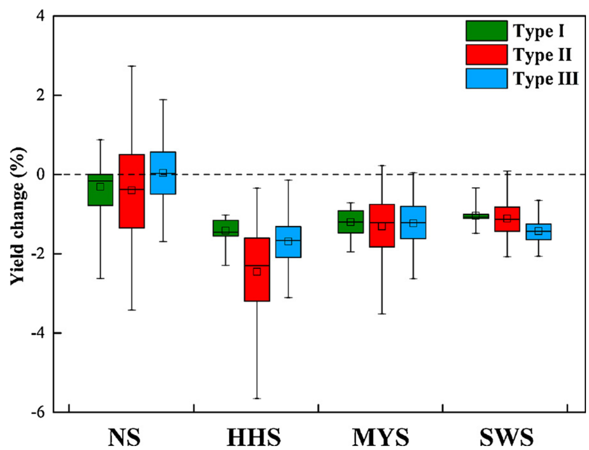

Fig. 7. Estimated yield change (%) for AFDD (accumulated frost degree-days) increased by 1 °C·d from stem elongation to flowering across stations in different sub-regions by using three types of model during 1981–2009. NS, the North Subregion, HHS, the Huang-Huai Subregion, MYS, the Middle-Lower Reaches of Yangzi River Subregion, SWS, the Southwest Subregion. In each box, going from bottom to top, horizontal lines represent the 5th percentile, 25th percentile, median, 75th percentile, and 95th percentile, and the open square represents the mean value.

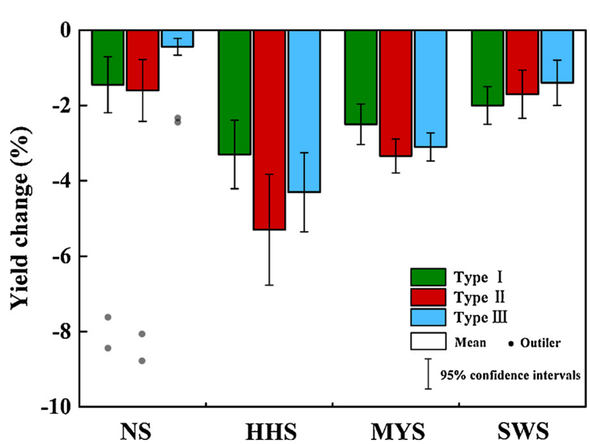

Fig. 8. Contribution of spring frost to yield change (%/year) during 1981–2009 at each sub-region. Whiskers show the 95% confidence interval. NS, the North Subregion, HHS, the Huang-Huai Subregion, MYS, the Middle-Lower Reaches of Yangzi River Subregion, SWS, the Southwest Subregion.

Despite other factors such as ice-nucleating bacteria, ice modifying proteins, soil type, and tissue structures (including awns, nodes, and crowns) affecting the direction and rate of ice nucleation, the physiological mechanism is not well understood (Gusta and Wisniewski, 2013). Because the actual frost and impact records, such as fungal infections, snow cover, and canopy temperature records are limited, it is difficult to scale them to larger geographic regions. Therefore, the Stevenson screen air temperatures quoted by meteorologists have been widely used for potential frost assessments at large scale (Crimp et al., 2016; Zheng et al., 2015). As described in the meteorological standard *Degree of Crop Frost Damage* (China Meteorological Administration, 2008), the surface temperatures of soil and plant below 0 °C or the Stevenson screen air temperatures lower than 2 °C can lead to a frost damage event. 2 °C air temperature measured by meteorological stations is commonly used as a frost threshold or an indicator of frost occurrence in most spring frost risk assessments (Crimp et al., 2014, 2016; Rebbeck and Knell, 2007; Zheng et al., 2015). Furthermore, we estimated yield responses with different temperature threshold ranges at different growth stages, revealing that 2 °C air temperature in the study period (GP2) was a reasonable temperature threshold to determine potential frost events (Fig. S4).

4.2. Spring frost sensitivity with different temperature thresholds

Frost disasters can be divided into different frost degrees according to different temperature thresholds. We tested the sensitivity of spring frost stress with different temperature threshold ranges (from -2 °C to 2 °C) during study period (Fig. S2). Our findings show that similar but weaker intensity and trends were observed with lower threshold temperatures (Fig. S2, Table S2). Similarly, the risk of spring frost occurrence greatly decreased when considering a –2 °C as threshold than a 2 °C in Australia (Crimp et al., 2016). It has been suggested that decreasing the threshold temperature from 0 °C to −1 °C in wheat could reduce frost-related yield loss, while little yield advantages was observed when the threshold temperature was below -2 °C (Zheng et al., 2015). Hence, developing wheat cultivar with high level of frost tolerance can escape spring frost and reduce frost-related yield loss. However, the difficulty in identifying useful reproductive resistance in wheat makes cultivars screening challenging (Frederiks et al., 2015).

4.3. Spatial and temporal variation of spring frost

Spring frost during stem elongation and flowering frequently occurred during 1981–2009 across most of the winter wheat-growing region of China. The estimated frost events with different temperature thresholds were still more severe in HHS (Fig. S2); this is why recent frost assessments have paid special attention to the Huang-Huai winter wheat sub-region (110 °E–118 °N and 34 °N–36 °N) among the main winter wheat-growing region (Song et al., 2006; Zhong et al., 2008, 2007b). In this region, the advantaged growth during the stem elongation stage because of global warming, coincided with a strong warm and cold fluctuation, is regarded as the main factor to cause the increasing spring frost events (Li et al., 2005). Additionally, the flat

topography of the Huang-Huai Plain wheat belt in HHS makes cold waves easily expand across this region (Zhong et al., 2008, 2007b). Yue et al. (2016) argued that frost was prone to occur in NS because cold air generally flows from Mongolia (northwest of China). However, our results focus on the period after the stem elongation stage which period in NS comes later and escapes some spring frost events accordingly. Zhou and Ren (2012) also pointed out that the frequencies of cold events decreased more significantly in northern China because of urbanization effect. The risk of frost damage in temperate regions has been getting increasing attention under climate change in recent years (Crimp et al., 2014; Li et al., 2015a), suggesting that global warming could result in the increasing risk of frost damage to crops in the south of China. Both winter warming and spring freeze occurred 3–8 times in each decade from 1961 to 2000 in Jiangsu province (temperate region), which seems a paradox (Li et al., 2015a). A similar result has been found in other temperate region, which the frost events in Southeast of Australia increased significantly (Crimp et al., 2014, 2016; Zheng et al., 2015). Temperature fluctuation is projected to trigger and exacerbate more extreme low temperature events (Gu et al., 2008; Li et al., 2015b). Our results showed that higher value of the temperature-drop-rate (TDR) in northern areas of study region but a rapid increase of TDR appeared in the south, suggesting that the high risk areas for frost stress expanded to the south, especially in the southeast (Anhui and Jiangsu provinces, ranking the country's top five wheat-producing provinces in China (National Bureau of Statistics of China, 2015)).

The actual temporal trends of spring frost stress is not exclusively attributed to temperature change but also to the variation of crop phenology shifting (Gu et al., 2008). The frost-sensitive stages coming earlier actually increases the risk of spring frost for crops and other species (Gu et al., 2008; Eccel et al., 2009). Actual risk of spring frost have not decreased as expected, although average temperature increasing have reduced spring frost significantly in most of wheat-growing region (Figs. 5 and 6, Table 4). Higher temperatures accelerate crop growth rates, but the variation of phenology shifting is not only mechanistically linked to temperature variation (Li et al., 2016a; He et al., 2015). Our results show the effects of phenology shifting to the trends of spring frost is disproportionately related to the effects of temperature variation at different stations, resulting in the actual trends of spring frost could not show distinct geographic distribution around the study region, which makes spring frost pattern become more complex and unpredictable (Fig. 5). Winter wheat phenology shifting can be affected by other factors including cultivar changes and agronomic management (Li et al., 2016a; Tao et al., 2012; Wang et al., 2013; Ying, 2013). In most wheat-growing regions in China, farmers have adapted to warming by changing sowing dates or planting alternative cultivars to manage wheat growth duration (Liu and Yuan, 2010; Wang et al., 2013). Ultimately, the phenology shifting over the past decades appears to be key growth stages advanced. For example, the vegetative growth period decreased by 2 days per decade in the North China Plain from 1981 to 2005 (White et al., 2011). Heading dates advanced significantly at about 40% of the locations across China during 1981–2007 (Tao et al., 2012). In other regions of the world, the beginning of heading dates in wheat are now significantly earlier, with a mean advance of 0.21 days per year during 1951–2004 in Germany (Estrella et al., 2007), and the trend of earlier heading or flowering dates were 0.8–1.8 days per decade during 1935–2004 in the U.S. Great Plains (Hu et al., 2005). We found that the starting date of stem elongation advanced at about half of the considered locations. Despite phenology shifting slightly increases the trends of frost stress, it counteracts the effects of temperature increasing to the trends of frost stress and causes actual frost trends remain the same or even increase (Table 4). Therefore, spring frost during the study period is still a potential threat on wheat production. To alleviate the effects of accelerated development, postponing the frost sensitive stage with a delayed sowing date or using cultivars with extended winter dormancy could be possible strategies to escape spring frost and minimize frost damage (Zheng et al., 2012). However, such adaption delays flowering and maturity dates, which increase the risk of exposing wheat to more heat stress or drought stress during grain filling (Liu et al., 2014; Zheng et al., 2012). If a delayed phenology date passes an optimum flowering and grain-filling period, more yield reduction could occur despite a reduced frost risk (Frederiks et al., 2012). Hence, managing phenology to balance both frost and heat risk is necessary. Defining region-specific sowing and flowering windows might be needed for each sub-region; these windows can be defined as the risk being less than 10% for frost (< 2 °C) between stem elongation and flowering and less than 30% for heat (> 30 °C) around flowering, similar to Zheng et al. (2012).

4.4. The impact of spring frost on winter wheat yield and uncertainties

Yield loss caused by frost generally depends on the intensity of the low temperature and its duration (Zhang et al., 2013). The previous studies have shown that the increase in daily minimum temperature can reduce cold injury (Wang et al., 2011; Zhou and Ren, 2012), and benefit wheat yield in China (Fang et al., 2015; Tao et al., 2017). However, the index of minimum temperature cannot capture the accumulated damage of extreme low temperature. A comprehensive index (accumulated frost degree-days, AFDD) defined in this study with both considering the intensity and duration of frost damage serves an effective way to evaluate frost stress and its impact on wheat yield. Both linear fixed-effects model and linear mixed model have shown a negative response of winter wheat grain yield to spring frost. For each 1 °C·d increase in AFDD, grain yields declined 7% in the entire winter wheat-growing region of China (Table 5). Chen et al. (2016) pointed that the impacts of climatic stress might have the opposite spatial patterns with their exposures. In contrast, our results showed that the higher exposures of spring frost in HHS coincided with higher sensitivities, with 1.7%–2.1% yield reduction for each 1 °C·d increase of AFDD (Table 5). In this region, spring frost contributed to 5% yield reduction per year more than other three regions during 1981–2009 (Fig. 8), suggesting spring frost stress in HHS poses the most threat to winter wheat yield. Winter wheat are often subject to multiple climatic stress during their growth period that lead to multiple influence on their yield (Tao et al., 2016; Trnka et al., 2014; Zhang et al., 2017a). Based on panel multiple regression approach, we analyzed the impacts of multiple climatic hazards and separated the impact of spring frost from them. The variance inflation factor (VIF) test (Table S3) and correlation analysis (Fig. S5) have shown that there are no multicollinearity among predictor variables in our models. Results were similar when using stepwise function for each type of models to select the input variables. Post-anthesis heat stress posed an adverse impact on wheat yield in most parts of China (Chen et al., 2016; Liu et al., 2014), which was consistent with our results (Table S1). Compared to the increasing trend of heat stress, winter wheat had lower exposure to spring frost (Liu et al., 2014; Zhang et al., 2017a), but higher sensitivity to spring frost was observed in our study (Table S1). Owing to the limited historical sample size, we further tested the potential uncertainties of frost impacts among different regions and different types of models (Figs. 7 and 8). Generally, the two northern regions have higher uncertainties than two southern regions. Precipitation or radiation is also reported to be a very important climate factor regulating crop yields and need to be separated from the effects of extreme temperature stress (Lobell et al., 2011; Tao et al., 2017, 2016). Simulation errors can arise if there is strong temporal correlation between temperature and precipitation or radiation (Lobell and Ortiz-Monasterio, 2007; Lobell and Burke, 2008). We applied multivariate linear regression to project precipitation responses and did not diagnose significant impact from precipitation on winter wheat yield in most of region (Table S1). This is mainly because our experiments had received well irrigation. Additionally, the model of type II have higher uncertainties than type I (Figs. 7 and 8). Fisher et al. (2012) indicated that measurement error will amplify if statistical models include too many 'fixed-effects' to control for possible omitted variables. To address this

problem, Carter et al (2016) applied linear mixed-effects models to separate heat stress from moisture stress, which set random effects on location, year and cultivar to control yield variance to management, regional, inter-annual and genetic factors. In making this comparison, we view location and year as random effects. The estimate values of spring frost impacts on winter wheat yield from linear mixed model (type III) was smaller than that calculated from linear fixed model (type II). Despite the model performance was improved when using mixed model, the uncertainty did not decrease. No information on cultivar shifts of yield dataset in different years and at different locations may account for the uncertainties of our model results. Other reason for uncertainties in winter wheat response to frost stress is that different soil types, soil moistures and plant population densities which were not considered in this study can change the actual perceived temperature for a crop (Rebbeck and Knell, 2007; Siebert et al., 2014; Whaley et al., 2004).

4.5. Remaining challenges in the future

Although a warmer climate is anticipated (Zhang et al., 2017b), the future shifts in spring frost events were not correlated with future climate scenarios (Zheng et al., 2012). Untimely radiation frost events in spring remain a problem and regularly cause serious damage to wheat production under future climate, especially in 2030 with a low-emission scenario (A2) (Zheng et al., 2012). Accelerated wheat phenology due to climate warming will counteract any positive effect of increasing minimum temperatures on frost-related yield in the future (Gu et al., 2008). For the high-emission and dry scenario, rising drought and elevated CO_2 will reinforce frost damage and limit wheat regrowth and recovery after frost damage (Bertrand et al., 2007; Niu et al., 2014). Therefore, separating the confounding effects for possible impacts and quantify the future impacts of spring frost on wheat production will be critical for developing appropriate adaptation strategies to spring frost.

Acknowledgements

This work was supported by the National Key Research and Development Program of China (2017YFD0300205), the National Science Foundation for Distinguished Young Scholars (31725020), the National Natural Science Foundation of China (31301234), the Priority Academic Program Development of Jiangsu Higher Education Institutions (PAPD), the 111 project (B16026), and China Scholarship Council.

Appendix A. Supplementary data

Supplementary material related to this article can be found, in the online version, at doi:https://doi.org/10.1016/j.agrformet.2018.06.006.

References

Akaike, H., 1987. Factor analysis and AIC. Psychometrika 52 (3), 317–332.
Al-Issawi, M., Rihan, H., El-Sarkassy, N., Fuller, M., 2013. Frost hardiness expression and characterisation in wheat at ear emergence. J. Agron. Crop Sci. 199 (1), 66–74.
Bao, Y., Wang, Y., Gao, P., Shen, S., 2012. Occurrence pattern on Spring frost injury of winter wheat in Jiangsu Province and its climatic risk division. Chin. J. Agrometeorol. 33 (1), 134–141.
Barlow, K., Christy, B., O'Leary, G., Riffkin, P., Nuttall, J., 2013. Simulating the impact of extreme heat and frost events on wheat production: the first steps. 20th International Congress on Modelling and Simulation. Modelling and Simulation Society of Australia and New Zealand Adelaide. pp. 545–551.
Bergjord, A.K., Bonesmo, H., Skjelvåg, A.O., 2008. Modelling the course of frost tolerance in winter wheat: I. Model development. Eur. J. Agron. 28 (3), 321–330.
Bertrand, A., Prévost, D., Bigras, F.J., Castonguay, Y., 2007. Elevated atmospheric CO 2 and strain of rhizobium alter freezing tolerance and cold-induced molecular changes in alfalfa (Medicago sativa). Ann. Bot. 99 (2), 275–284.
Carter, E.K., Melkonian, J., Riha, S.J., Shaw, S.B., 2016. Separating heat stress from moisture stress: analyzing yield response to high temperature in irrigated maize. Environ. Res. Lett. 11 (9), 094012.
Chen, L.J., Xiang, H.Z., Miao, Y., Zhang, L., Guo, Z.F., Zhao, X.H., Lin, J.W., Li, T.L., 2014. An overview of cold resistance in plants. J. Agron. Crop Sci. 200 (4), 237–245.
Chen, Y., Zhang, Z., Wang, P., Song, X., Wei, X., Tao, F., 2016. Identifying the impact of multi-hazards on crop yield—a case for heat stress and dry stress on winter wheat yield in northern China. Eur. J. Agron. 73, 55–63.
China Meteorological Administration, 2008. QX/T 88-2008. Grade of Crop Frost Damage. China Standards Press, Beijing (in Chinese).
Crimp, S., Bakar, K.S., Kokic, P., Jin, H., Nicholls, N., Howden, M., 2014. Bayesian space–time model to analyse frost risk for agriculture in Southeast Australia. Int. J. Climatol.
Crimp, S., Zheng, B., Khimashia, N., Gobbett, D., Chapman, S., Howden, M., Nicholls, N., 2016. Recent changes in Southern Australian frost occurrence: implications for wheat production risk. Crop Pasture Sci. 8 (67), 801–811.
Eccel, E., Rea, R., Caffarra, A., Crisci, A., 2009. Risk of spring frost to apple production under future climate scenarios: the role of phenological acclimation. Int. J. Biometeorol. 53 (3), 273–286.
Estrella, N., Sparks, T.H., Menzel, A., 2007. Trends and temperature response in the phenology of crops in Germany. Glob. Change Biol. 13 (8), 1737–1747.
Fang, S., Cammarano, D., Zhou, G., Tan, K., Ren, S., 2015. Effects of increased day and night temperature with supplemental infrared heating on winter wheat growth in North China. Eur. J. Agron. 64, 67–77.
FAO., 2016. http://www.fao.org/.
Feng, Y.X., He, W.X., Sun, Z.F., Zhong, X.L., 1999. Climatological study on frost damage of winter wheat in China. Acta Agron. Sin. 25 (3), 335–340.
Fisher, A.C., Hanemann, W.M., Roberts, M.J., Schlenker, W., 2012. The economic impacts of climate change: evidence from agricultural output and random fluctuations in weather: comment. Amer. Econ. Rev. 102 (7), 3749–3760.
Fowler, D., Carles, R., 1979. Growth, development, and cold tolerence of fall-acclimated cereal grains 1. Crop Sci. 19 (6), 915–922.
Fowler, D., Limin, A., Wang, S.-y., Ward, R., 1996. Relationship between low-temperature tolerance and vernalization response in wheat and rye. Can. J. Plant Sci. 76 (1), 37–42.
Frederiks, T., Christopher, J., Harvey, G., Sutherland, M., Borrell, A., 2012. Current and emerging screening methods to identify post-head-emergence frost adaptation in wheat and barley. J. Exp. Bot. 63 (15), 5405–5416.
Frederiks, T.M., Christopher, J.T., Sutherland, M.W., Borrell, A.K., 2015. Post-head-emergence frost in wheat and barley: defining the problem, assessing the damage, and identifying resistance. J. Exp. Bot. 66 (12), 3487–3498.
Fuller, M.P., Fuller, A.M., Kaniouras, S., Christophers, J., Fredericks, T., 2007. The freezing characteristics of wheat at ear emergence. Eur. J. Agron. 26 (4), 435–441.
Gu, L., Hanson, P.J., Mac Post, W., Kaiser, D.P., Yang, B., Nemani, R., Pallardy, S.G., Meyers, T., 2008. The 2007 eastern US spring freeze: increased cold damage in a warming world? BioScience 58 (3), 253–262.
Gusta, L.V., Wisniewski, M., 2013. Understanding plant cold hardiness: an opinion. Physiol. Plant 147 (1), 4–14.
He, L., Asseng, S., Zhao, G., Wu, D., Yang, X., Zhuang, W., Jin, N., Yu, Q., 2015. Impacts of recent climate warming, cultivar changes, and crop management on winter wheat phenology across the loess plateau of China. Agr. For. Meteorol. 200, 135–143.
Holman, J.D., Schlegel, A.J., Thompson, C.R., Lingenfelser, J.E., 2011. Influence of precipitation, temperature, and 56 years on winter wheat yields in Western Kansas. Crop Manage. 2011 (4), 1–15.
Hu, Q., Weiss, A., Feng, S., Baenziger, P.S., 2005. Earlier winter wheat heading dates and warmer spring in the US Great plains. Agr. For. Meteorol. 135 (1), 284–290.
IPCC, 2012. Managing the Risks of Extreme Events and Disasters to Advance Climate Change Adaptation. Cambridge University Press., Cambridge, UK, Cambridge University Press, Cambridge, UK.
Jin, S., 1996. Wheat in China. China Agricultural Press, Beijing.
Li, M., Wang, D., Zhong, X., 2005. Current situation and prospect of research on frost of winter wheat. J. Nat. Disasters 14 (4), 72.
Li, X., Cai, J., Liu, F., Dai, T., Cao, W., Jiang, D., 2014. Cold priming drives the subcellular antioxidant systems to protect photosynthetic electron transport against subsequent low temperature stress in winter wheat. Plant Physiol. Biochem. 82, 34–43.
Li, X., Cai, J., Liu, F., Dai, T., Cao, W., Jiang, D., 2015a. Spring freeze effect on wheat yield is modulated by winter temperature fluctuations: evidence from meta-analysis and simulating experiment. J. Agron Crop. Sci. 201 (4), 288–300.
Li, X., Cai, J., Liu, F., Zhou, Q., Dai, T., Cao, W., Jiang, D., 2015b. Wheat plants exposed to winter warming are more susceptible to low temperature stress in the spring. Plant Growth Regul. 77 (1), 11–19.
Li, X., Pu, H., Liu, F., Zhou, Q., Cai, J., Dai, T., Cao, W., Jiang, D., 2015c. Winter wheat photosynthesis and grain yield responses to spring freeze. Agron. J. 107 (3), 1002–1010.
Li, K., Yang, X., Tian, H., Pan, S., Liu, Z., Lu, S., 2016a. Effects of changing climate and cultivar on the phenology and yield of winter wheat in the North China Plain. IJBm 60 (1), 21–32.
Li, X., Jiang, D., Liu, F., 2016b. Winter soil warming exacerbates the impacts of Spring Low temperature stress on wheat. J. Agron. Crop Sci. 202 (6), 554–563.
Liu, Y.J., Yuan, G.F., 2010. Impacts of climate change on winter wheat growth in Panzhuang irrigation District, Shandong Province. J. Geogr. Sci. 20 (6), 861–875.
Liu, X., Zhang, Z., Shuai, J., Wang, P., Shi, W., Tao, F., Chen, Y., 2013. Impact of chilling injury and global warming on rice yield in Heilongjiang Province. J. Geogr. Sci. 23 (1), 85–97.
Liu, B., Liu, L., Tian, L., Cao, W., Zhu, Y., Asseng, S., 2014. Post-heading heat stress and yield impact in winter wheat of China. Glob. Change Biol. 20 (2), 372–381.
Lobell, D.B., Ortiz-Monasterio, J.I., 2007. Impacts of day versus night temperatures on spring wheat yields: A comparison of empirical and CERES model predictions in three

locations. Agron. J. 99 (2), 469–477.
Lobell, D.B., Burke, M.B., 2008. Why are agricultural impacts of climate change so uncertain? The importance of temperature relative to precipitation. Environ. Res. Lett. 3 (3), 034007.
Lobell, D.B., Bänziger, M., Magorokosho, C., Vivek, B., 2011. Nonlinear heat effects on African maize as evidenced by historical yield trials. Nat. Clim. Change 1 (1), 42–45.
Majláth, I., Szalai, G., Soós, V., Sebestyén, E., Balázs, E., Vanková, R., Dobrev, P.I., Tari, I., Tandori, J., Janda, T., 2012. Effect of light on the gene expression and hormonal status of winter and spring wheat plants during cold hardening. Physiol. Plant 145 (2), 296–314.
Marcellos, H., Single, W., 1984. Frost injury in wheat ears after ear emergence. Funct. Plant Biol. 11 (2), 7–15.
Mueller, T., Pusuluri, N., Mathias, K., Cornelius, P., Barnhisel, R., Shearer, S., 2004. Map quality for ordinary kriging and inverse distance weighted interpolation. SSSAJ 68 (6), 2042–2047.
National Bureau of Statistics of China, 2015. China Statistical Yearbook 2015. http://www.stats.gov.cn/tjsj/ndsj/2015/indexch.htm.
Niu, S., Luo, Y., Li, D., Cao, S., Xia, J., Li, J., Smith, M.D., 2014. Plant growth and mortality under climatic extremes: an overview. Environ. Exp. Bot. 98, 13–19.
Porter, J.R., Gawith, M., 1999. Temperatures and the growth and development of wheat: a review. Eur. J. Agron. 10 (1), 23–36.
Prescott, J., 1940. Evaporation from a water surface in relation to solar radiation. Trans. R. Soc. S. Aust. 64 (1), 114–118.
Rebbeck, M., Knell, G., 2007. Managing Frost Risk: A Guide for Southern Australian Grains. South Australian Research and Development Institute.
Saeidi, M., Eliasi, P., Abdoly, M., Sasani, S., 2014. Freezing tolerance of wheat cultivars at the early growing season after winter. Afr. J. Biotechnol. 11 (17), 4045–4052.
Schauberger, B., Archontoulis, S., Arneth, A., Balkovic, J., Ciais, P., Deryng, D., Elliott, J., Folberth, C., Khabarov, N., Müller, C., 2017. Consistent negative response of US crops to high temperatures in observations and crop models. Nat. Commun. 8, 13931.
Schlenker, W., Roberts, M.J., 2009. Nonlinear temperature effects indicate severe damages to US crop yields under climate change. Proc. Natl. Acad. Sci. 106 (37), 15594–15598.
Shi, P., Tang, L., Wang, L., Sun, T., Liu, L., Cao, W., Zhu, Y., 2015. Post-heading heat stress in rice of South China during 1981-2010. PLoS One 10 (6) e0130642.
Shimono, H., 2011. Earlier rice phenology as a result of climate change can increase the risk of cold damage during reproductive growth in northern Japan. Agric. Ecosyst. Environ. 144 (1), 201–207.
Siebert, S., Ewert, F., Rezaei, E.E., Kage, H., Graß, R., 2014. Impact of heat stress on crop yield—on the importance of considering canopy temperature. Environ. Res. Lett. 9 (4), 044012.
Single, W., 1966. Studies on frost injury to wheat. III. Screening of varieties for resistance to ear and stem frosting. Crop Pasture Sci. 17 (5), 601–610.
Single, W., 1984. Frost injury and the physiology of the wheat plant. J. Aust. Inst. Agric. Sci. 51 (2), 128–134.
Song, Y., Chen, D., Dong, W., 2006. Influence of climate on winter wheat productivity in different climate regions of China, 1961-2000. Clim. Res. 32 (3), 219.
Stone, M., 1974. Cross-validatory choice and assessment of statistical predictions. J. R. Stat. Soc. Ser. B (Methodol.) 111–147.
Tack, J., Barkley, A., Nalley, L.L., 2015. Effect of warming temperatures on US wheat yields. Proc. Natl. Acad. Sci. 112 (22), 6931–6936.
Tao, F., Zhang, S., Zhang, Z., 2012. Spatiotemporal changes of wheat phenology in China under the effects of temperature, day length and cultivar thermal characteristics. Eur J. Agron. 43, 201–212.
Tao, F., Zhang, Z., Shi, W., Liu, Y., Xiao, D., Zhang, S., Zhu, Z., Wang, M., Liu, F., 2013. Single rice growth period was prolonged by cultivars shifts, but yield was damaged by climate change during 1981-2009 in China, and late rice was just opposite. Glob. Chang Biol. 19 (10), 3200–3209.
Tao, F., Zhang, Z., Zhang, S., Rötter, R.P., 2015. Heat stress impacts on wheat growth and yield were reduced in the Huang-Huai-Hai Plain of China in the past three decades. Eur. J. Agron. 71, 44–52.
Tao, F., Zhang, Z., Zhang, S., Rötter, R.P., 2016. Variability in crop yields associated with climate anomalies in China over the past three decades. Reg. Environ. Change 1–9.
Tao, F., Xiao, D., Zhang, S., Zhang, Z., Rötter, R.P., 2017. Wheat yield benefited from increases in minimum temperature in the Huang-Huai-Hai Plain of China in the past three decades. Agr For. Meteorol. 239, 1–14.
Trnka, M., Rötter, R.P., Ruiz-Ramos, M., Kersebaum, K.C., Olesen, J.E., Žalud, Z., Semenov, M.A., 2014. Adverse weather conditions for European wheat production will become more frequent with climate change. Nat. Clim. Change 4 (7), 637.
Valluru, R., Link, J., Claupein, W., 2012. Consequences of early chilling stress in two Triticum species: plastic responses and adaptive significance. Plant. Biol. 14 (4), 641–651.
Wang, X., Piao, S., Ciais, P., Li, J., Friedlingstein, P., Koven, C., Chen, A., 2011. Spring temperature change and its implication in the change of vegetation growth in North America from 1982 to 2006. Proc. Natl. Acad. Sci. 108 (4), 1240–1245.
Wang, J., Wang, E., Feng, L., Yin, H., Yu, W., 2013. Phenological trends of winter wheat in response to varietal and temperature changes in the North China Plain. Field Crop Res. 144, 135–144.
Wang, P., Zhang, Z., Song, X., Chen, Y., Wei, X., Shi, P., Tao, F., 2014. Temperature variations and rice yields in China: historical contributions and future trends. Clim. Change 124 (4), 777–789.
Wang, H., Vicente-serrano, S.M., Tao, F., Zhang, X., Wang, P., Zhang, C., Chen, Y., Zhu, D., Kenawy, A.E., 2016. Monitoring winter wheat drought threat in Northern China using multiple climate-based drought indices and soil moisture during 2000–2013. Agr. For. Meteorol. 228–229, 1–12.
Whaley, J.M., Kirby, E.J.M., Spink, J.H., Foulkes, M.J., Sparkes, D.L., 2004. Frost damage to winter wheat in the UK: the effect of plant population density. Eur J. Agron. 21 (1), 105–115.
White, J.W., Kimball, B.A., Wall, G.W., Ottman, M.J., Hunt, L., 2011. Responses of time of anthesis and maturity to sowing dates and infrared warming in spring wheat. Field Crop Res. 124 (2), 213–222.
Wu, Y., Zhong, X., Hu, X., Ren, D., Lv, G., Wei, C., Song, J., 2014. Frost affects grain yield components in winter wheat. N. Z. J. Crop Hortic. Sci. 42 (3), 194–204.
Ying, H., 2013. Winter wheat phenological phases and its responses to climate changes in Eastern Henan. Guizhou Agric. Sci. 9, 042.
Yue, Y., Zhou, Y., Wang, Ja., Ye, X., 2016. Assessing wheat frost risk with the support of GIS: an approach coupling a growing season meteorological index and a hybrid fuzzy neural network model. Sustainability 8 (12), 1308.
Zhang, T., Zhu, J., Wassmann, R., 2010. Responses of rice yields to recent climate change in China: an empirical assessment based on long-term observations at different spatial scales (1981–2005). Agr For. Meteorol. 150 (7), 1128–1137.
Zhang, Z., Liu, X., Wang, P., Shuai, J., Chen, Y., Song, X., Tao, F., 2013. The heat deficit index depicts the responses of rice yield to climate change in the northeastern three provinces of China. Reg. Environ. Change 1–12.
Zhang, Z., Wang, P., Chen, Y., Zhang, S., Tao, F., Liu, X., 2014. Spatial pattern and decadal change of agro-meteorological disasters in the main wheat production area of China during 1991–2009. J. Geogr. Sci. 24 (3), 387–396.
Zhang, J., Zhang, Z., Tao, F., 2017a. Performance of temperature-related weather index for agricultural insurance of Three Main crops in China. Int. J. Disaster Risk Sci. 1–13.
Zhang, T., Wang, J., Teng, Y., 2017b. Adaptive effectiveness of irrigated Area expansion in mitigating the impacts of climate change on crop yields in Northern China. Sustainability 9 (5), 851.
Zhang, L., Zhang, Z., Chen, Y., Wei, X., Song, X., 2018. Exposure, vulnerability, and adaptation of major maize-growing areas to extreme temperature. Nat. Hazards 1–16.
Zheng, B., Chenu, K., Fernanda Dreccer, M., Chapman, S.C., 2012. Breeding for the future: what are the potential impacts of future frost and heat events on sowing and flowering time requirements for Australian bread wheat (Triticum aestivium) varieties? Glob. Change Biol. 1365–2486.
Zheng, B.Y., Chapman, S.C., Christopher, J.T., Frederiks, T.M., Chenu, K., 2015. Frost trends and their estimated impact on yield in the Australian wheatbelt. J. Exp. Bot. 66 (12), 3611–3623.
Zhong, X., Wang, D., Li, Y., 2007a. Risk assessment of frost damage in wheat. J. Appl. Meteorol. Sci. 18 (1), 102–107.
Zhong, X., Wang, D., Zhao, P., Yan, X., Su, C., 2007b. Occurrence of frost temperature in Huanghuai wheat production zone after winter wheat elongation. Chin. J. Eco-Agric. 5, 003.
Zhong, X., Mei, X., Li, Y., Yoshida, H., Zhao, P., Wang, X., Han, L., Hu, X., Huang, S., Huang, J., 2008. Changes in frost resistance of wheat young ears with development during jointing stage. J. Agron. Crop Sci. 194 (5), 343–349.
Zhou, Y., Ren, G., 2012. Change in extreme temperature event frequency over mainland China, 1961-2008. Clim. Res. 50 (2), 125.